Sensors & Actuators: B. Chemical 345 (2021) 130445

Contents lists available at ScienceDirect

Sensors and Actuators: B. Chemical

journal homepage: www.elsevier.com/locate/snb

A distance-based paper sensor for rapid detection of blood lactate concentration using gold nanoparticles synthesized by *Satureja hortensis*

Younes Mirzaei [a], Ali Gholami [a,*], Mohammad Mahdi Bordbar [b]

[a] *Department of Analytical Chemistry, Faculty of Chemistry, University of Kashan, Kashan, 87317-51167, Iran*
[b] *Personal Laboratory, Fasa, 74614, Iran*

ARTICLE INFO

Keywords:
Microfluidic instrument
Colorimetric detection
Lactate
Green synthesis
Distance measurement
Biofluids

ABSTRACT

Rapid detection of lactate as the major fuel source and material to support the level of blood sugar can open up a new class of analysis for nutritionists and sports medicine practitioners. Here, a rapid and user-friendly method for monitoring changes in the blood lactate concentration is reported, involving the use of a paper strip coated with gold nanoparticles (AuNPs). The aqueous extract of *Satureja hortensis* is used as the reduction agent in a green synthesis of the AuNPs. Due to the interaction between the NPs and lactate flowing across the paper strip, they change color from red to purple, which can be detected by the naked eye. It is possible to create a distance-based paper sensor, representing these changes as a column of colored bars on the paper substrate whose length has a good linear relationship with the lactate concentration ranged between 1.0 and 30.0 mM. By recording the color changes with a scanner, the sensor response is also obtained using an image analysis method, leading to a linear calibration curve in the lactate concentration range of 0.5–30.0 mM. The resulting detection limits of the lactate measurements are found to be 0.6 and 0.47 using the distance measurement and image analysis methods, respectively. Interestingly, in the presence of interfering species, the sensor is selective for lactate, while also showing good performance in measuring the lactate concentration in the real blood samples.

1. Introduction

Changes in the blood lactate concentration can be used as a criterion for assessing diseases in human body [1–4]. The lactate ion results from an anaerobic glycoside reaction that is eventually metabolized in the liver, and excreted [1,2]. The lactate concentration in a healthy person's blood should be in the range of 0.5–2.2 mM but some activities such as heavy exercise or pulmonary embolism change the ion balance, so that the excessive lactate will be accumulated in the blood as it cannot be dehydrogenated [5,6]. In this regard, serious injuries including liver, kidney, and cardiovascular insufficiencies may occur for lactate concentrations higher than 4 mM [7–10]. Moreover, in the case of acute conditions, the high lactate concentration may lead to the growth of cancerous tumors [5]. Therefore, the lactate concentration needs to be monitored and determined rapidly and accurately, especially for individuals who perform strenuous exercise (e.g., bodybuilding athletes).

Commonly, the lactate concentration measurement methods are divided into the following three categories: chromatography coupled by mass spectroscopy, proton nuclear magnetic resonance, and enzyme-based spectrophotometry [11–15]. Although these methods provide reliable results by being sensitive and selective to lactate, they are required to be equipped with advanced devices, which in turn involve the use of expensive reagents to perform the tests. Besides from their time-consuming sample preparation techniques, a professional operator is also needed to procure the data, and interpret the results. To overcome these limitations, biosensors utilizing the enzyme lactate dehydrogenase have been proposed, being capable of oxidizing lactate to pyruvate [16]. In other words, the biosensors convert the nicotinamide adenine dinucleotide (NAD^+) to its reduced form (NADH), which can be detected by electrochemical and colorimetric methods [16]. Although the biosensing method is simple and has appropriate selectivity compared to the instrumental methods, the cost of fabrication and keeping of these sensors are not affordable. Moreover, environmental changes can reduce the activity of the enzyme, giving rise to adverse effects on the sensor performance [17].

The alternative approach would be to utilize colorimetric sensors whose sensing elements involve the use of organic compounds, mineral reagents and metal nanoparticles (NPs) [18]. The presence of specific functional groups in the structure of these materials can lead to a chemical reaction based on the lock-and-key theory [19]. The process of

* Corresponding author.
E-mail address: agholami@kashanu.ac.ir (A. Gholami).

https://doi.org/10.1016/j.snb.2021.130445
Received 24 March 2021; Received in revised form 26 June 2021; Accepted 13 July 2021
Available online 14 July 2021

sensor fabrication is simple and cost-effective. Because the method is based on color change which is visible to the naked eye, it is very popular among users. Also, these methods can be named as on-site and on-time assay [20,21]. The Among them, sensors fabricated using metal NPs have shown higher sensitivity and selectivity, arising from unique electrical and optical properties of the NPs [22]. For example, the molar absorption coefficient of NPs is 10^4 times higher than that of organic dye reagents [23]. This feature, along with their high surface to volume ratio, enables NPs to detect extremely small concentrations of the analyte [23]. Furthermore, it is possible to modify the surface of NPs with different chemical and biological compounds, thereby inducing the occurrence of different electrostatic, covalent, hydrogen or nucleophilic interactions between the analyte and the active sites of the coating agent [24]. The type and combination ratio of the coating agents with the NPs can affect morphology, size and surface charge of the resultant NPs, enhancing the selectivity to a particular analyte [25].

Essentially, NPs can be prepared based on chemical and green synthetic approaches [26]. Despite the chemical approach by which NPs are synthesized with the help of toxic, carcinogenic and environmentally harmful chemicals, the green approach is inexpensive and simple by employing safe substances such as plant extracts, tissues, microorganisms, etc [27]. In fact, plant extracts are mostly used in the green approach due to their high availability and cost-effective preparation [27]. Meanwhile, green NPs have shown good antibacterial and anticonvulsant properties, leading to less harmful effects on human health and the environment [26].

Conventionally, clinical methods for lactate detection are carried out in well-plates made of glass with low safety, consuming large amounts of materials including reagents, enzymes and analytes [28]. Today, several paper-based methods have been developed to identify and measure metabolites, performing the experiment on a paper substrate that is accessible, biocompatible and portable [29]. Accordingly, the paper-based methods can be used as a point of care device, being designed in lateral flow, microfluidic and origami structures [30].

Nevertheless, sensors performing based on the measurement of the stain length have become more popular, involving the formation of a color stain due to the interaction between the analyte and the reagent on the paper surface [31]. In fact, the stain length can be measured using a ruler, being proportional to the analyte concentration [32]. Evidently, the aforementioned distance-based method does not require the use of external reading tools. While this method has already been employed in various applications such as measuring the concentration of metal ions [33,34] and anions [35], no reports are available on the use of distance-based paper sensors for the detection of blood lactate concentration, according to the best of our knowledge.

In this paper, a stain length measurement technique is used for qualitative and quantitative analysis of the lactate concentration by fabricating a sensor whose sensing element is made of Au NPs synthesized by a green method. The reduction agent used in the AuNPs synthesis is the aqueous extract of summer savory plant (*Satureja hortensis*), being rich in phenolic acids such as rosmarinic, caffeic, isoferulic, paracoumaric, sinapic and chlorogenic acids [36]. This reduces Au (III) to Au (0), while also forming hydrogen bonds with lactate functional groups, which can give rise to the aggregation of AuNPs. The resulting interaction between the NPs and lactate leads to the creation of a stain on the paper substrate that can be observed both visually and with the help of a ruler. The advantage of the present study is that the distance-based analysis is coupled with measurements based on the image processing, thus reducing human error in detecting the stain length, and achieving reliable sensing results. Since the interaction between the NPs and lactate is expected to be influenced by environmental and chemical factors, their effect on the sensor response is investigated from the distance measurement and image analysis methods. Under optimal conditions, the sensor is used for the quantitative measurement of lactate in the real blood samples.

2. Experimental details

2.1. Materials

The materials used in this study were pure and be in analytical grades. Whatman Grade NO.2 filter paper was purchased to fabricate the paper based sensor. The leaves of *Satureja hortensis* were provided from Kashan local market. Gold (III) chloride trihydrate ($HAuCl_4.3H_2O$) and the other chemical compounds such as sodium lactate ($NaC_3H_5O_3$), sodium nitrate ($NaNO_3$), potassium nitrate (KNO_3), calcium nitrate tetrahydrate ($Ca(NO_3)_2.4H_2O$), magnesium nitrate hexahydrate ($Mg(NO_3)_2{\cdot}6\ H2O$), sodium nitrite ($NaNO_2$), sodium carbonate (Na_2CO_3), sodium sulfate (Na_2SO_4), sodium phosphate (Na_3PO_4), sodium thiocyanate (NaSCN), uric acid, histidine, creatinine, lysine, tyrosine, cysteine, glucose, ascorbic acid, L-alanine, glycine, hydrochloric acid (HCl), phosphoric acid (H_3PO_4), acetic acid (CH_3COOH), tris-hydroxymethyl methane (Tris), boric acid (H_3BO_3) were obtained from Sigma Aldrich Company. Lactate stock solutions with the concentration of 35 mM was prepared for experimental procedures.

2.2. Equipment

The synthesis of NPs were verified by some instrumental methods such as UV–vis (OPTIZEN 3220UV, South Korea), FT-IR (Perklin-Elmer781). The size and the surface electrical charge of NPs were calculated by using Zetasizer Nano ZS90 (Malvern, UK). Field emission scanning electron microscopy (FE-SEM; MIRA3 TESCAN) and SEM-attached energy dispersed spectroscopy (EDX) were used to evaluate the fabricating sensor process. The photos of PAD were recorded by a flatbed scanner (CanoScanLiDE 700F, with a resolution of 300 dpi, USA). Image J software (1.51n, National Institutes of Health, USA) (https://imagej.nih.gov/ij/download.html) was applied to analyze the sensor images.

2.3. Synthesis of AuNPs

To synthesize AuNPs, the method proposed by Gharehyakheh was used with some modifications [37]. Initially, the leaves of summer savory plant was rinsed with distilled water, and then placed at room temperature for several days to dry. The dried leaves was well ground in a mortar. Afterwards, 10.0 mg of the resultant powder was poured into 100.0 mL of boiled water, and the mixture was stirred vigorously for 1 h. To remove the plant residues, the mixture was filtered with filter paper, followed by twice centrifugation at 3900 rpm for 20 min. The supernatant was then filtered using a syringe filter (0.22 μm) and it was repeated several times to obtain a colorless solution. The resulting solution was diluted 10 times with double-distilled water, and used as the reducted agent in the subsequent synthesis of Au NPs. In this respect, 100.0 mL of aqueous $HAuCl_4$ solution with a concentration of 1.0×10^{-3} M was heated up to the boiling point. Afterwards, 10.0 mL of the diluted extract was added dropwise to the boiling solution under vigorous stirring. The solution color changed gradually from yellow to tomato red, confirming the synthesis of AuNPs.

2.4. Design of the paper sensor

Whatman Grade 2 filter paper was cut in the dimension of 0.5×3 cm using a cutter. This piece of paper was immersed in a mixture containing AuNPs and a Britton-Robinson buffer for 10 s, thereby completely covering the surface of the paper with the NPs. The prepared sensor was stuck on a double-sided tape whose one side was attached to a pad, and other side was attached to a glass slide as the holder. In fact, the double-sided tape hydrophobized the pad, preventing the NPs or analyte from spreading outside it. A calibrated bar was also placed on the right side of the pad to act as a ruler, measuring the length of the stain. For better clarity, Fig. 1 schematically shows the design of the

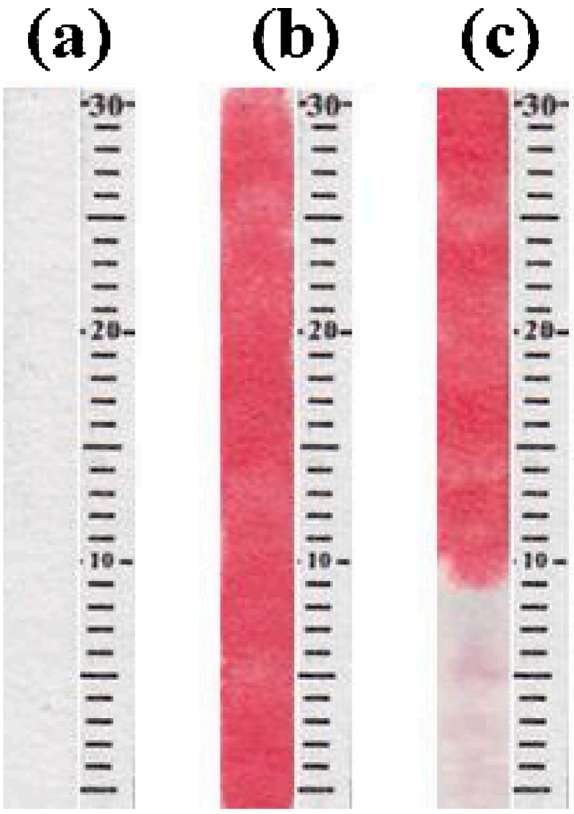

Fig. 1. The images of (a) the fabricated PAD, (b) the PAD after immersing in the gold NPs solution, and (c) The PAD after exposing to lactate (4.0 mM). (For interpretation of the references to colour in this figure text, the reader is referred to the web version of this article.)

paper sensor.

2.5. Lactate concentration detection by the distance-based method

40.0 μL of standard lactate solution with a specified concentration was added to the sensor from the bottom width of the pad. Due to the capillary nature of the paper, the lactate flowed along the paper, interacting with the NPs while also causing the paper to change color from red to purple. Depending on the lactate concentration, the lactate ion flowed into a certain distance on the surface of the paper. This distance was measured using the ruler placed on the pad. The measurement criterion in this method is the lowest red spot that remains on the paper strip and has not changed color. The calibration curve was obtained by plotting the measured distance as a function of lactate concentration.

2.6. Lactate concentration detection by the image analysis method

The color change in the paper substrate can be measured using image analysis software such as Image J. Accordingly, using a scanner, the sensor image was initially obtained before and after the interaction, selecting its entire rectangular area. Numerical values were calculated pixel by pixel for red, green and blue color components, then, the average numerical value of each color component was obtained. The mean values calculated before and after the interaction were subtracted from each other, thus preparing a column of colored bar representing the sensor response. On the other hand, the subtracted values were used to calculate the Euclidean (norm) as follows:

$$Euclidean\ norm = \sqrt{(\Delta R)^2 + (\Delta G)^2 + (\Delta B)^2} \quad (1)$$

where ΔR, ΔG and ΔB are the subtracted values of red, green and blue color components, respectively. The numerical value of the Euclidean norm was the final response of the sensor through the image analysis, enabling us to plot a calibration curve.

2.7. Clinical analysis of lactate in a real sample

Lactate was measured in a real sample using enzyme-based methods in a medical diagnostic laboratory [28]. The lactate dehydrogenase enzyme can convert lactate and NAD^+ to pyruvate and NADH, respectively. The resultant NADH was measured by a spectrophotometer at a wavelength of 340 nm, representing the lactate concentration in the blood. To this end, a sterilized tube was initially weighed empty. 6.0 mL of metaphosphoric acid (3.0 g/dL) was then added to the tube, and weighted again. 2.0 mL of blood sample was mixed with the metaphosphoric acid in a tube. The weights of the tube and the mixture were measured. To calculate the dilution factor (D), Eq. (2) was employed as given below:

$$D = \frac{W_m - W_e}{W_m - W_a} \quad (2)$$

where W_m is the weight of the tube containing the mixture, W_e is the weight of the empty tube, and W_a is the weight of the tube containing the acid. In order to achieve a homogeneous mixture, the sample was kept in an ice container for 10 min. The mixture was then centrifuged at 3000 rpm for 15 min, followed by separating the supernatant from the mixture. In continuance, three cuvettes were used as the control sample, calibration sample and test sample, and filled with 0.1 mL of metaphosphoric acid (3.0 g/dL), 0.1 mL of lithium lactate and 0.1 mL of supernatant, respectively. 30.0 μL of lactate dehydrogenase (2.0 mg/mL) and 200 μL of NAD^+ (2.7×10^{-2} M) were added to each cuvette. The resultant mixture was then stirred on a shaker for 20 min. Afterwards, using the control sample, the absorption was set to zero at the wavelength of 340 nm. Meanwhile, the absorption of the calibration and test samples was recorded at the wavelength of 340 nm. To calculate the lactate concentration (mM), the following equation was used:

$$Lactate\ concentration = \frac{Absorption\ of\ test\ sample \times D}{Absorption\ of\ calibration\ sample} \quad (3)$$

2.8. Analysis of lactate in a real sample by the proposed sensor

In order to evaluate the sensor performance for detecting lactate in a real sample, a plasma sample was prepared from a medical diagnostic laboratory, and 10 standard lactate concentrations were added to it.

Each sample was then divided into two parts: one part was analyzed by the clinical method, and the other part was analyzed by the proposed sensor. In this respect, 40.0 μL of the lactate-containing plasma sample was injected into the pad. The resultant color changes were evaluated by both the distance measurement and image analysis methods. On the other hand, 40.0 μL of the lactate-free plasma sample was injected into the pad as the control sample. The responses obtained for the control sample were subtracted from those for the test samples. To find the lactate concentration in the plasma sample, the net response of the sensor was substituted in the calibration equation. Using statistical parameters, concentration values obtained by the proposed sensor were also compared with those by the clinical method. The schematic diagram of the proposed procedure were summarized in Scheme 1.

3. Results and discussion

3.1. UV–vis, FT-IR and DLS of AuNPs

The UV–vis spectrum of the AuNPs is shown in Fig. S1a, indicating that they have a maximum absorption at 525 nm. FT-IR spectroscopy was also used to identify functional groups present at the NP surface. To this end, FT-IR spectrum of the *Satureja hortensis* extract was compared

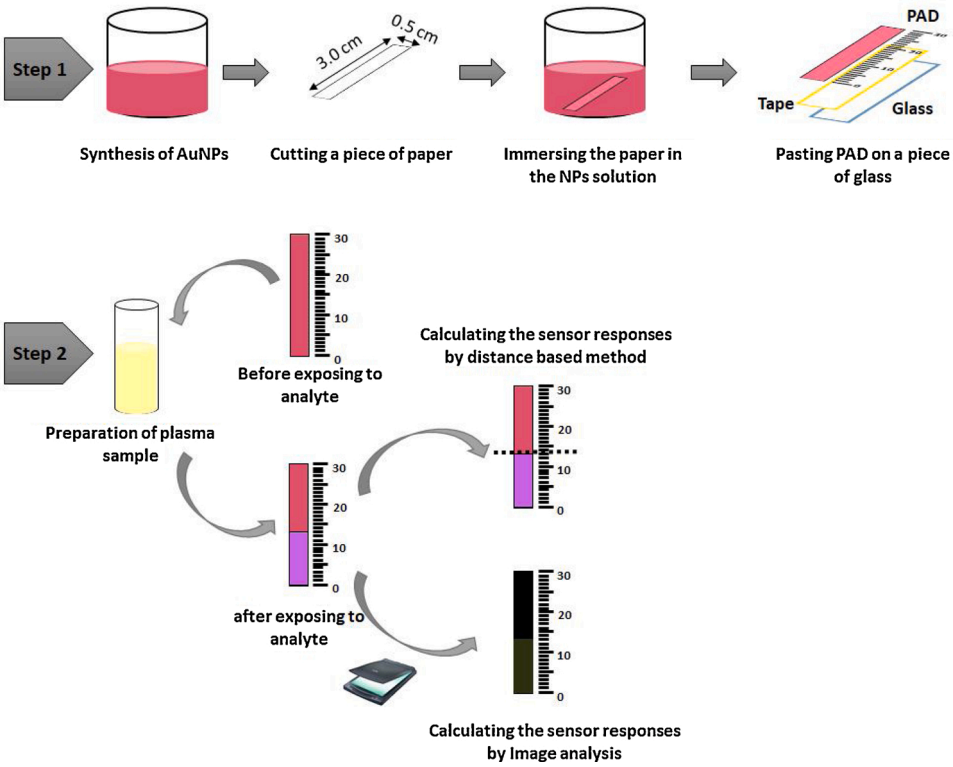

Scheme 1. The schematic diagram of experimental procedure for detection of lactate ions in this study.

with that of the synthesized AuNPs, and the results are shown Fig. S1b. As can be seen, the main peaks in the FT-IR spectrum of the extract are mostly observed in the AuNP spectrum. However, they have lower intensities, and are shifted toward higher wave numbers, confirming the synthesis of the AuNPs using the *Satureja hortensis* extract. The peak at 3400 cm^{-1} is attributed to the alcoholic and phenolic OH stretching vibrations, whereas NH amide stretching vibrations are responsible for the appearance of the peak at 3000 cm^{-1}. Moreover, the peak at 2800 cm^{-1} arises from the CH stretching vibrations of alkanes. The emergence of the peaks in the wave number ranges of 2200–2100 cm^{-1}, and 1630–1610 cm^{-1} can be assigned to C≡C and C≡N groups in aromatic and aliphatic compounds, and C═C and C═O groups in aromatic compounds and proteins, respectively. It should be noted that the peaks relating to the CO bending vibrations range from 1100 to 1200 cm^{-1}, arising from alkanes, alcohols, carboxylic acids, esters and ethers [38].

Fig. S1c shows hydrodynamic size distribution histogram of the AuNPs obtained by the DLS method. It is found that the average size of the NPs synthesized by the green approach is 38 nm. The surface charge of the AuNPs was also calculated by the zero potential method, and the results are shown in Fig. S1d. The corresponding load distribution histogram indicates that the surface of the NPs is negatively charged (−14 mV).

3.2. FE-SEM and EDX of the sensor

Surface modification of the Whatman paper with the AuNPs was investigated by FE-SEM and EDX analyses. As shown in Fig. S2a, the Whatman paper is made of a series of cellulose fibers. Following the immersion of the paper in the solution containing AuNPs, they become homogeneously distributed on the surface, according to Fig. S2b. The corresponding EDX spectrum depicted in Fig. S2d shows a strong peak at 2.3 keV, confirming the presence of the element Au in the nanoparticle structure coated on the paper.

To investigate the repeatability of the sensor fabrication, five cut pieces of paper were immersed in a solution containing AuNPs, and then stuck on a double-sided tape. The mean values of red, green and blue color components were calculated for each sensor. In the next step, the relative standard deviation (RSD %) value of each color component was obtained, and the results are presented in Table S1. The low RSD values indicate that the fabrication process of the distance-based paper sensor has good repeatability.

3.3. Optimization of the sensor

Since a mixture of the buffer and AuNPs was used in the fabrication of the sensor, some parameters such as the NP volume, solution pH, buffer type, buffer concentration, analyte volume, and the interaction time between the analyte and the sensor are expected to affect the sensor response. Therefore, the aforementioned parameters need to be optimized in order to obtain the highest sensor response for the lactate concentration measurement.

The optimization process of the sensor response in the present study was calculated for both the distance measurement and image analysis methods. In the first experiment, the proposed sensor was prepared by immersing a cut piece of paper in a mixture of the buffer and different NP volumes in the range of 2.0–10.0 μL. The interaction between lactate and AuNPs was investigated for each of the fabricated sensor, and the results are shown in Fig. 2a. As observed, the sensor response increases with increasing the NP volume, reaching a maximum value at the volume of 8.0 μL. Note that the sensor response is not affected by NP volumes higher than this volume. Therefore, the sensor was prepared by immersing the cut piece of paper in a mixture of 10.0 μL of buffer, 8.0 μL of Au NPs, and 2.0 μL of double-distilled water.

In the second experiment, the sensor response was evaluated under different acidic and alkaline conditions by changing the pH of the mixture from 4.0 to 12.0. According to Fig. 2b, the highest sensor response is obtained at pH = 8.0. Essentially, an undesirable sensor response may be caused by active site protonation at low pH values and/or hydroxyl ion interference and electron repulsion at more alkaline pH values [23].

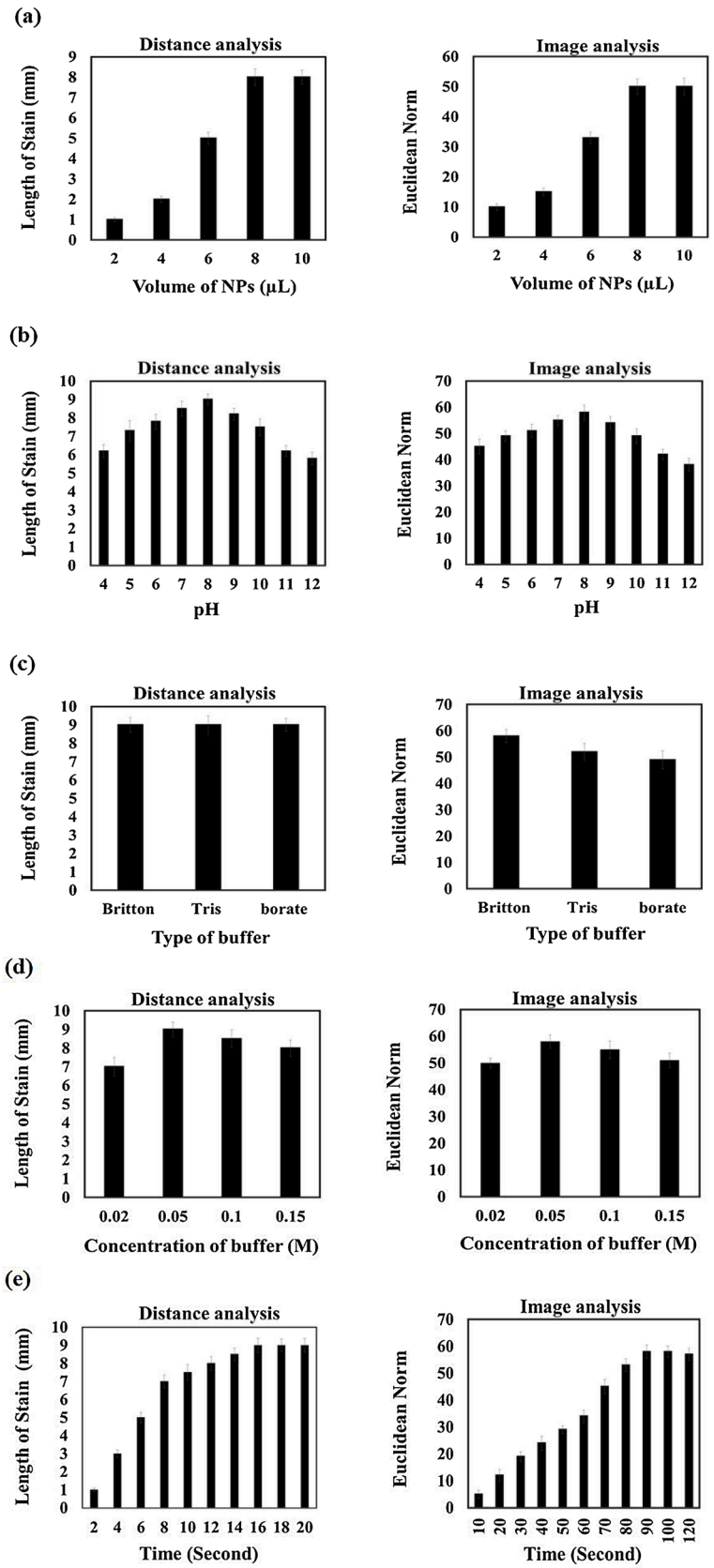

Fig. 2. Optimization process. Evaluation the effect of (a) volume of NPs, (b) pH of media, (c) type of buffer, (d) buffer concentration and (e) incubation time on the response of sensor in the presence of lactate (4.0 mM).

The interaction between lactate and the sensor was investigated for three different buffer solutions, including Britton-Robinson buffer, Tris buffer and Borate buffer. The experiment was carried out at the optimal pH = 8.0. Fig. 2c shows that, while the sensor response calculated by the distance measurement is the same for the different buffer types, the image analysis method indicates that the highest sensor response results from the Britton-Robinson buffer. In order to keep the experiment conditions the same for the both analyses, the Britton-Robinson buffer was also used for the subsequent analyses.

In continued, the effect of buffer concentration on the sensor response was evaluated by changing the selected buffer concentration in the range of 0.02–0.15 M. The corresponding results presented in Fig. 2d indicate that the interaction between lactate and the sensing element is enhanced with increasing the buffer concentration from 0.02 to 0.05 M. At higher concentrations, the sensor response is reduced due to the presence of other ionic species as well as the ion-ion interference [24].

At the end, the time required to perform a complete reaction between the analyte and the sensor was assessed. This time was calculated from the moment of analyte injection until reaching reaction equilibrium between lactate and AuNPs. However, according to Fig. 2e, the results indicate that the analyte travels a distance of 9 mm in 16 s (based on distance analysis), but the interaction between lactate and nanoparticles reaches equilibrium after 90 s (based on image analysis).

3.4. The sensor response mechanism

Fig. 1(c) shows the response of the proposed sensor to lactate with a concentration of 4.0 mM. As can be seen, the color of AuNPs changes from red to purple as a result of their interaction with lactate. The sensor response mechanism can be explained by the fact that the summer savory aqueous extract is rich in the phenolic acids, comprising phenolic and carboxylic groups. Since lactate consists of an alcohol group and an acidic group, an esterification reaction can occur between the acidic group of lactate and the alcohol groups of the acids in the extract. Similarly, an esterification reaction may take place between the lactate alcohol group and the extract acidic groups, thus forming a bridge between the AuNPs [36]. In this way, the distance between the NPs is reduced, leading to their aggregation on the paper surface. In this regard, FE-SEM image depicted in Fig. 2Sc evidences the aggregated AuNPs due to their interaction with lactate.

3.5. Quantitative measurement of lactate

The proposed sensor was used to measure lactate with different concentrations. In this regard, an aqueous solution of lactate was initially prepared with the different concentrations in the range of 0.0–30.0 mM. Afterwards, 40.0 µL of each solution was added to the pad separately, and lactate and the sensor were allowed to interact with each other. The corresponding sensor response is shown in Fig. 3a. As observed, the interaction between lactate and AuNPs causes the sensor to change color from red to purple. The length of the purple stain produced on the sensor substrate is proportional to the analyte concentration. With an increase in the concentration, lactate can move further on the surface of the paper. The calibration curve shown in Fig. 4a indicates a linear relationship between the distance moved and the lactate concentration in the range of 1.0–30.0 mM. It is worth noting that the theoretical detection limit for this measurement was calculated to be 0.6 mM.

Using the image analysis, the color change of the sensor was calculated before and after the interaction with lactate, and subtracted from each other. Fig. 3b presents the subtracted values as a color map, comprising two distinct parts: a colored part, and a black part. The former represents the occurrence of interaction, and the latter indicates the absence of interaction between lactate and AuNPs. The color maps confirm the results obtained by the distance measurement analysis. For each color map, the Euclidean norm was calculated, representing the net

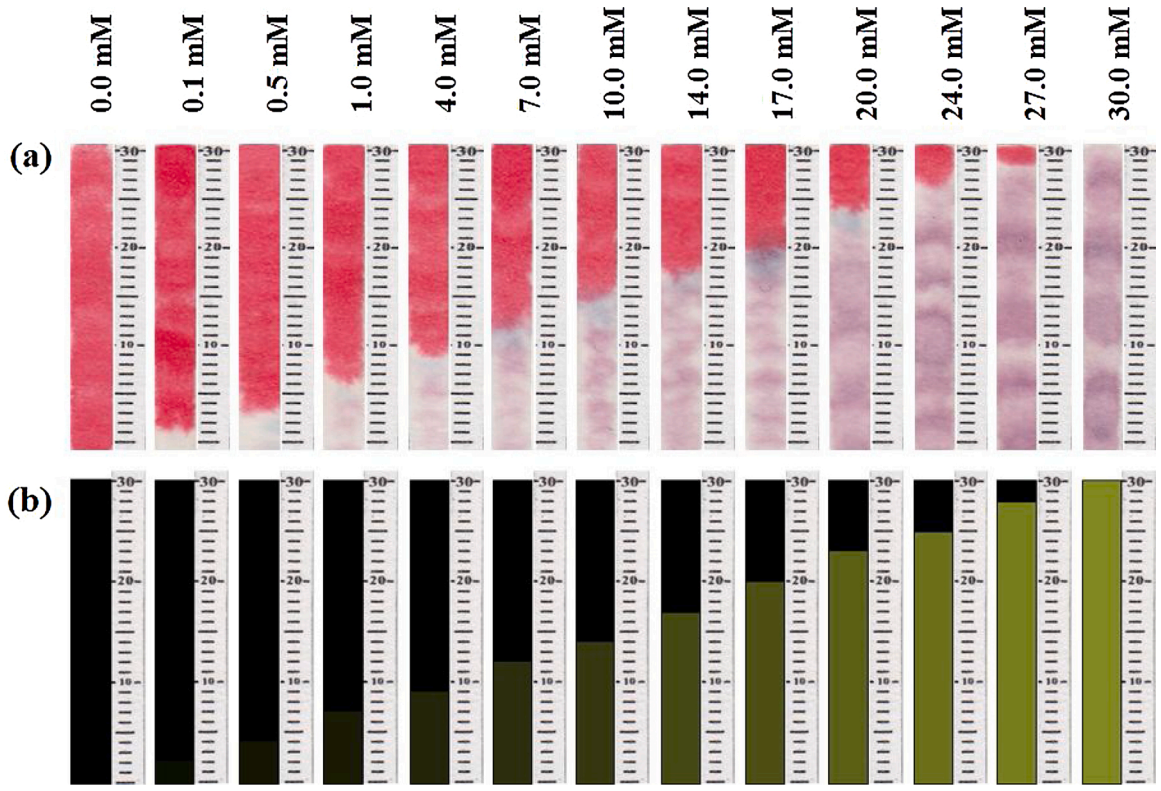

Fig. 3. The sensor responses (a) and the respective color maps (b) for different concentrations of lactate. The sensor was fabricated by mixing 8.0 µL of NPs by 10.0 µL of Britton-Robinson buffer (pH 8.0, 0.05 M) and 2.0 µL double-distilled water. The results were collected after 1.5 min. (For interpretation of the references to colour in this figure text, the reader is referred to the web version of this article.)

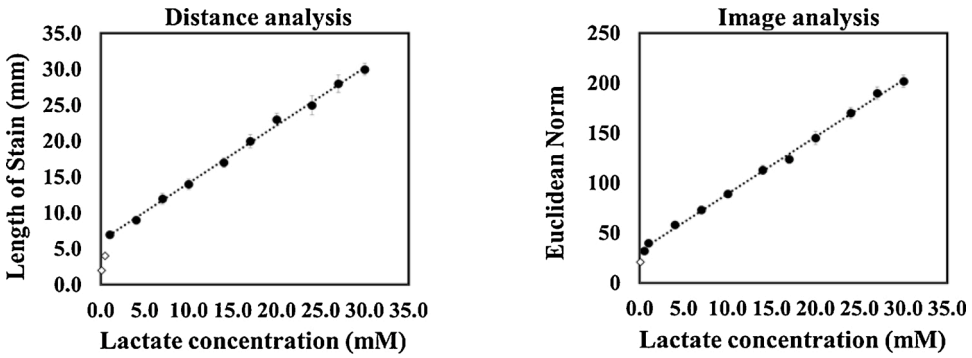

Fig. 4. The calibration plot obtained by distance and image analysis. The concentration of lactate varied from 0.0 to 30.0 mM. The sensor was fabricated by mixing 8.0 μL of NPs by 10.0 μL of Britton-Robinson buffer (pH 8.0, 0.05 M) and 2.0 μL double-distilled water. The results were collected after 1.5 min.

sensor response. Accordingly, a calibration curve was obtained by plotting the Euclidean norm against lactate concentration, as shown in Fig. 4b. The calibration curve is found to be linear in the range of 0.5–30.0 mM, giving rise to a detection limit of 0.47 mM. Table 1 presents the analytical information obtained from both the distance measurement and image analysis methods. As inferred, the image analysis shows a better sensitivity rather than the distance analysis. Moreover, a better correlation is found between the lactate concentrations and the results obtained using the image analysis method. Nevertheless, the distance measurement method is a faster, simpler and more user-friendly method compared to the image analysis.

3.6. Sensor reproducibility

To ensure that the sensor can provide reproducible responses, 5 separate sensors were prepared, and injected with lactate with a concentration of 4.0 mM. The results were calculated in the form of stain length and Euclidean norm, as presented in the bar graphs of Fig. S3. The RDS values of the distance measurement and image analysis methods are obtained to be 4.60 % and 4.39 %, respectively. In this way, the paper sensor response is reproducible, arising from the low RSD values.

3.7. Interference effect

Since interfering species might be present in real samples, the selectivity of the proposed sensor to lactate was investigated as follows: Initially, solutions of different compounds such as ions [e.g., sodium, potassium, magnesium (II) and calcium (II)], anions (e.g., chloride, nitrate, nitrite, carbonate, phosphate, thiocyanate and sulfate), amino acids (e.g., histidine, lysine, cysteine, tyrosine, Glycine and alanine) and other chemicals (e.g., glucose, creatinine and ascorbic acid) were prepared. The solutions were then mixed separately with lactate at concentration ratios of 1000, 100, 50 and 25. It should be noted that the lactate concentration in all the prepared mixtures was constant to 4.0 mM. The sensor responses for the mixtures were compared with those for only lactate, and the results are presented in Table 2. Evidently, at least up to 25 times of the lactate concentration, most of the species used in the present study were not interferences for lactate determinations.

Table 1
The figures of merit for quantitative analysis of lactate.

Figures of merit	Assay-based on Distance analysis	Assay-based on Image analysis
Linear range (mM)	1.0−30.0	0.5−30.0
Detection Limit (mM)	0.6	0.47
Calibration equation	R = 0.81 C + 6.10	R = 5.69 C + 32.34
R^2	0.997	0.998
Calibration sensitivity	0.81	5.69
Analytical sensitivity (for 28 mM)	0.66	0.92

Table 2
Evaluating the effect of interfering species on the sensor responses.

Interferences	Tolerance Limit[a] ([Interferences]/[Lactate])
Na^+, K^+, Mg^{2+}, Ca^{2+}, Cl^-, NO_3^-, NO_2^-, CO_3^{2-}, PO_4^{3-}, SO_4^{2-}	1000
SCN^-, Uric acid, Histidine, Creatinine	100
Lysine, Tyrosine, cysteine, Glucose, Ascorbic acid	50
L-alanine, Glycine	25

[a] Tolerance Limit is a specified concentration of interferences in the presence of analyte that provide a relative error less than 5 %.

3.8. Evaluation of the sensor stability

The effect of environmental factors on the stability of the proposed sensor was investigated by monitoring the color changes for a specific period of time using the image analysis method. As shown in Fig. S4, no changes in the sensor color is observed for up to 15 days. However, after that period of time, the sensor is not stable against temperature and chemical changes, leading to the progressive aggregation of the AuNPs. Of course, if the sensor was kept in a suitable package with the presence of a dehumidifier and the same temperature conditions, the stability of the sensor against environmental factors will definitely increase. This time can even be extended 5 months.

In another experiment, the response of an as-fabricated sensor was compared with that of a 15 and 150 day old sensor in the presence of lactate using the distance measurement and image analysis methods. The results obtained are presented in Table S2. According to the statistical calculations, no significant difference is found between the responses of the two sensors, so that one can use them for a period of 15 days (when the sensor stored in the outdoor condition) or 150 days (when the sensor stored in the sealed package) in order to efficiently analyze the lactate concentration.

3.9. Practical analysis

As previously explained in Section 2.7, the proposed sensor was used to measure lactate in a plasma sample. Table 3 presents the comparison between the results obtained from the paper sensor and the standard method. The recovery and relative error of the sensor are indicative of its high accuracy and validity for measuring lactate in plasma samples, giving rise to a reliable diagnostic method. Interestingly, by adding plasma without the lactate sample, no changes was observed in the sensor responses obtained by both distance determination and image analysis. Therefore, in this experiment, the sensor detected only to

Table 3
Comparison the results of clinical, distance and image analyses for determination of lactate in the real samples.

Sample	Added (mM)	Clinical analysis		Distance analysis			Image analysis		
		Founded[a] (mM)	Recovery (%)	Founded[a] (mM)	Recovery (%)	Relative error[b] (%)	Founded[a] (mM)	Recovery (%)	Relative error[b] (%)
1 (without lactate)	0	0	–	0	–	–	0	–	–
2 (with lactate)	0	1.80 (±0.047)	–	1.92 (±0.096)	–	6.66	1.90 (±0.077)	–	5.55
3	2.0	3.69 (±0.081)	97	3.91 (±0.179)	100	5.98	3.86(±0.161)	99	4.84
4	4.0	5.92 (±0.184)	102	5.63(±0.240)	95	−4.74	5.65(±0.240)	96	−4.47
5	6.0	7.88 (±0.228)	101	7.43(±0.386)	94	−5.69	7.49(±0.362)	95	−4.91
6	8.0	9.99 (±0.349)	102	9.37(±0.453)	94	−6.12	9.44(±0.387)	95	−5.47
7	10.0	11.56 (±0.277)	98	12.39 (±0.664)	104	7.25	12.26 (±0.614)	103	6.14
8	12.0	13.38 (±0.441)	97	14.24 (±0.729)	102	6.47	14.14 (±0.670)	102	5.74
9	14.0	16.27 (±0.472)	103	17.38(±0.792	109	6.84	17.31 (±0.799)	109	6.41
10	16.0	18.16 (±0.653)	102	17.16 (±0.866)	96	−5.46	17.20 (±0.732)	96	−5.28
11	18.0	19.40 (±0.601)	98	18.58 (±0.955)	93	−4.18	18.36 (±0.908)	92	−5.32

[a] The average of three repetitive determinations (±SD).
[b] Relative error was calculated between the mean values obtained by the proposed sensor and the clinical analysis.

lactate ions.

On the other hand, Table S3 presents the analytical parameters obtained by different methods for measuring lactate. Although the enzymatic methods show higher sensitivity, the enzyme-free method proposed in the present study utilizes NPs synthesized with the plant extract, considerably lowering the preparation cost of the sensing element compared to the enzymes. Also, in addition to the simple coating of the NPs on the paper substrate, the proposed sensor does not require specific keeping conditions. Compared to other methods, the distance measurement and image analysis methods used here do not need laboratory conditions, operators and expensive reading devices, providing an almost wide linear range along with a better detection limit. Each paper strip costs just $ 0.5 to make, which means it's affordable and can be used by anyone.

4. Conclusions

In conclusion, a green NP-based colorimetric method was proposed for measuring lactate. The resulting color change was investigated using the three following methods: naked-eye observation, stain length measurement, and image analysis. The experiment was carried out on a piece of paper, employing a smaller amount of the sensing element and analyte compared to conventional methods. The proposed sensor was capable of detecting small amounts of lactate with good selectivity in the presence of interfering species. The results obtained indicate that the distance measurement method can be a suitable candidate for monitoring lactate in blood samples. However, the image analysis method showed better sensitivity in the quantitative measurements. The responses of the real sample indicate that the proposed sensor can replace the enzymatic method used for measuring lactate in the blood sample of people with diabetes, and liver failure. Moreover, using the paper sensor, it is possible to investigate the lactate levels in the blood of athletes, thereby evaluating the exercise intensity and the training method performed. Despite all the advantages, the designed sensor is not stable for a long time against environmental conditions. It is disposable and is not reversible. If the method was not coupled with the image analysis, calculation of the sensor responses can be associated with errors by using the distance quantification method.

CRediT authorship contribution statement

Younes Mirzaei: Methodology, Investigation, Writing - original draft. **Ali Gholami:** Conceptualization, Supervision, Writing - review & editing. **Mohammad Mahdi Bordbar:** Methodology, Validation.

Declaration of Competing Interest

The authors report no declarations of interest.

Acknowledgments

The authors gratefully acknowledge the financial support from the Kashan University Research Council.

Appendix A. Supplementary data

Supplementary material related to this article can be found, in the online version, at doi:https://doi.org/10.1016/j.snb.2021.130445.

References

[1] G.A. Brooks, The science and translation of lactate shuttle theory, Cell Metab. 27 (2018) 757–785, https://doi.org/10.1016/j.cmet.2018.03.008.
[2] G. Kemp, D. Böning, G. Strobel, R. Beneke, N. Maassen, R.A. Robergs, F. Ghiasvand, D. Parker, Lactate accumulation, proton buffering, and pH change in ischemically exercising muscle, Am. J. Physiol. - Regul. Integr. Comp. Physiol. 289 (2005), https://doi.org/10.1152/ajpregu.00641.2004.
[3] S. Hughes, Early lactate clearance is associated with improved outcome in severe Sepsis and septic shock, J. Intensive Care Soc. 6 (2005) 36–37, https://doi.org/10.1177/175114370500600222.
[4] F. Valenza, G. Aletti, T. Fossali, G. Chevallard, F. Sacconi, M. Irace, L. Gattinoni, Lactate as a marker of energy failure in critically ill patients: Hypothesis, Crit. Care 9 (2005) 588–593, https://doi.org/10.1186/cc3818.
[5] B. Faubert, K.Y. Li, L. Cai, C.T. Hensley, J. Kim, L.G. Zacharias, C. Yang, Q.N. Do, S. Doucette, D. Burguete, H. Li, G. Huet, Q. Yuan, T. Wigal, Y. Butt, M. Ni, J. Torrealba, D. Oliver, R.E. Lenkinski, C.R. Malloy, J.W. Wachsmann, J.D. Young, K. Kernstine, R.J. DeBerardinis, Lactate metabolism in human lung tumors, Cell 171 (2017) 358–371, https://doi.org/10.1016/j.cell.2017.09.019, e9.
[6] Y. Hu, H. Cheng, X. Zhao, J. Wu, F. Muhammad, S. Lin, J. He, L. Zhou, C. Zhang, Y. Deng, P. Wang, Z. Zhou, S. Nie, H. Wei, Surface-enhanced Raman scattering active gold nanoparticles with enzyme-mimicking activities for measuring glucose and lactate in living tissues, ACS Nano 11 (2017) 5558–5566, https://doi.org/10.1021/acsnano.7b00905.
[7] Brajesh Singh, Saikat K. Jana, Nilanjana Ghosh, Soumen K. Das, Mamata Joshi, Parthasarathi Bhattacharyya, Koel Chaudhury, Metabolomic profiling of doxycycline treatment in chronic obstructive pulmonary disease, J. Pharm. Biomed. Anal. 132 (2017) 103–108, https://doi.org/10.1016/j.jpba.2016.09.034.
[8] G.D. Lopaschuk, Metabolic modulators in heart disease: past, present, and future, Can. J. Cardiol. 33 (2017) 838–849, https://doi.org/10.1016/j.cjca.2016.12.013.
[9] M.M. Sayeed, P.N.A. Murthy, Adenine nucleotide and lactate metabolism in the lung in endotoxin shock, Circ. Shock 8 (1981) 657–666.
[10] R. Bellomo, Bench-to-bedside review: lactate and the kidney, Crit. Care 6 (2002) 322–326, https://doi.org/10.1186/cc1518.

[11] M.P. Milagres, S.C.C. Brandão, M.A. Magalhães, V.P.R. Minim, L.A. Minim, Development and validation of the high performance liquid chromatography-ion exclusion method for detection of lactic acid in milk, Food Chem. 135 (2012) 1078–1082, https://doi.org/10.1016/j.foodchem.2012.05.047.
[12] J. Galbán, S. de Marcos, J.R. Castillo, Fluorometric-enzymatic lactate determination based on enzyme cytochrome b2 fluorescence, Anal. Chem. 65 (1993) 3076–3080, https://doi.org/10.1021/ac00069a022.
[13] S.B. Barker, William H. Summerson, The colorimetric determination of lactic acid in biological material, J. Biol. Chem. 138 (1941) 535–554. http://www.jbc.org/content/138/2/535.citation.
[14] F. Wu, Y. Huang, C. Huang, Chemiluminescence biosensor system for lactic acid using natural animal tissue as recognition element, Biosens. Bioelectron. 21 (2005) 518–522, https://doi.org/10.1016/j.bios.2004.10.029.
[15] D.P. Soares, M. Law, Magnetic resonance spectroscopy of the brain: review of metabolites and clinical applications, Clin. Radiol. 64 (2009) 12–21, https://doi.org/10.1016/j.crad.2008.07.002.
[16] J.P. Talasniemi, S. Pennanen, H. Savolainen, L. Niskanen, J. Liesivuori, Analytical investigation: assay of d-lactate in diabetic plasma and urine, Clin. Biochem. 41 (2008) 1099–1103, https://doi.org/10.1016/j.clinbiochem.2008.06.011.
[17] M.M. Bordbar, T.A. Nguyen, F. Arduini, H. Bagheri, Optoelectronic nose based on an origami paper sensor for selective detection of pesticide aerosols, Microchim. Acta. 187 (2020), https://doi.org/10.1007/s00604-020-04596-x.
[18] M.M. Bordbar, T.A. Nguyen, A.Q. Tran, H. Bagheri, Optoelectronic nose based on an origami paper sensor for selective detection of pesticide aerosols, Sci. Rep. 10 (2020), https://doi.org/10.1038/s41598-020-74509-8.
[19] L. You, D. Zha, E.V. Anslyn, Recent advances in supramolecular analytical chemistry using optical sensing, Chem. Rev. 115 (2015) 7840–7892, https://doi.org/10.1021/cr5005524.
[20] B. Kuswandi, Nuriman, J. Huskens, W. Verboom, Optical sensing systems for microfluidic devices: a review, Anal. Chim. Acta 601 (2007) 141–155, https://doi.org/10.1016/j.aca.2007.08.046.
[21] G.G. Morbioli, T. Mazzu-Nascimento, A.M. Stockton, E. Carrilho, Technical aspects and challenges of colorimetric detection with microfluidic paper-based analytical devices (μPADs) - A review, Anal. Chim. Acta 970 (2017) 1–22, https://doi.org/10.1016/j.aca.2017.03.037.
[22] M.M. Bordbar, J. Tashkhourian, B. Hemmateenejad, Structural elucidation and ultrasensitive analyses of volatile organic compounds by paper-based nano-optoelectronic noses, ACS Sens. 4 (2019) 1442–1451, https://doi.org/10.1021/acssensors.9b00680.
[23] M.M. Bordbar, B. Hemmateenejad, J. Tashkhourian, S.F. Nami-Ana, An optoelectronic tongue based on an array of gold and silver nanoparticles for analysis of natural, synthetic and biological antioxidants, Microchim. Acta 185 (2018), https://doi.org/10.1007/s00604-018-3021-1.
[24] A. Sheini, A paper-based device for the colorimetric determination of ammonia and carbon dioxide using thiomalic acid and maltol functionalized silver nanoparticles: application to the enzymatic determination of urea in saliva and blood, Microchim. Acta 187 (2020), https://doi.org/10.1007/s00604-020-04553-8.
[25] A. Vincenzo, P. Roberto, F. Marco, M.M. Onofrio, I. Maria Antonia, Surface plasmon resonance in gold nanoparticles: a review, J. Phys. Condens. Matter 29 (2017), 203002. http://stacks.iop.org/0953-8984/29/i=20/a=203002.
[26] V.K. Oxana, R.D. H.V, I.K. Boris, O.P. Betsabee, M.J.P. Victor, The greener synthesis of nanoparticles, Trends Biotechnol. 31 (2013) 240–247.
[27] M. Bandeira, M. Giovanela, M. Roesch-Ely, D.M. Devine, J. da Silva Crespo, Green synthesis of zinc oxide nanoparticles: a review of the synthesis methodology and mechanism of formation, Sustain. Chem. Pharm. 15 (2020), https://doi.org/10.1016/j.scp.2020.100223.
[28] A. Butch, Tietz textbook of clinical chemistry, Hum. Pathol. 26 (1995) 1391–1392, https://doi.org/10.1016/0046-8177(95)90313-5.
[29] D.M. Cate, J.A. Adkins, J. Mettakoonpitak, C.S. Henry, Recent developments in paper-based microfluidic devices, Anal. Chem. 87 (2015) 19–41, https://doi.org/10.1021/ac503968p.
[30] A. Sheini, Colorimetric aggregation assay based on array of gold and silver nanoparticles for simultaneous analysis of aflatoxins, ochratoxin and zearalenone by using chemometric analysis and paper based analytical devices, Microchim. Acta 187 (2020), https://doi.org/10.1007/s00604-020-4147-5.
[31] H. Shibata, Y. Hiruta, D. Citterio, Fully inkjet-printed distance-based paper microfluidic devices for colorimetric calcium determination using ion-selective optodes, Analyst 144 (2019) 1178–1186, https://doi.org/10.1039/c8an02146e.
[32] M. Taghizadeh-Behbahani, B. Hemmateenejad, M. Shamsipur, A. Tavassoli, A paper-based length of stain analytical device for naked eye (readout-free) detection of cystic fibrosis, Anal. Chim. Acta 1080 (2019) 138–145, https://doi.org/10.1016/j.aca.2019.06.050.
[33] L. Cai, Y. Fang, Y. Mo, Y. Huang, C. Xu, Z. Zhang, M. Wang, Visual quantification of Hg on a microfluidic paper-based analytical device using distance-based detection technique, AIP Adv. 7 (2017), https://doi.org/10.1063/1.4999784.
[34] M.P. Nguyen, S.P. Kelly, J.B. Wydallis, C.S. Henry, Read-by-eye quantification of aluminum (III) in distance-based microfluidic paper-based analytical devices, Anal. Chim. Acta 1100 (2020) 156–162, https://doi.org/10.1016/j.aca.2019.11.052.
[35] K. Phoonsawat, N. Ratnarathorn, C.S. Henry, W. Dungchai, A distance-based paper sensor for the determination of chloride ions using silver nanoparticles, Analyst 143 (2018) 3867–3873, https://doi.org/10.1039/c8an00670a.
[36] I. Fierascu, C.E. Dinu-Pirvu, R.C. Fierascu, B.S. Velescu, V. Anuta, A. Ortan, V. Jinga, Phytochemical profile and biological activities of satureja hortensis l.: a review of the last decade, Molecules 23 (2018), https://doi.org/10.3390/molecules23102458.
[37] S. Gharehyakheh, A. Ahmeda, A. Haddadi, M. Jamshidi, M. Nowrozi, M. M. Zangeneh, A. Zangeneh, Effect of gold nanoparticles synthesized using the aqueous extract of Satureja hortensis leaf on enhancing the shelf life and removing Escherichia coli O157:H7 and Listeria monocytogenes in minced camel's meat: the role of nanotechnology in the food indus, Appl. Organomet. Chem. 34 (2020), https://doi.org/10.1002/aoc.5492.
[38] I. Rasaee, M. Ghannadnia, S. Baghshahi, Biosynthesis of silver nanoparticles using leaf extract of Satureja hortensis treated with NaCl and its antibacterial properties, Microporous Mesoporous Mater. 264 (2018) 240–247, https://doi.org/10.1016/j.micromeso.2018.01.032.

Younes Mirzaei received his BSc in Applied Chemistry from the Islamic Azad University of Kazerun in 2009, and his MSc in Phytochemistry from Yasouj University in 2013. He has been a PhD student in Analytical Chemistry at Kashan University since 2016. His research has been in the field of isolation, purification, and identification of natural compounds of plants and algae as well as analysis of plant essential oils. He is currently active in the field of colorimetric sensors, and the production of paper-based analytical sensors.

Ali Gholami is an Assistant Professor of Chemistry at Chemistry Department of Kashan University. He received his BSc in Applied Chemistry from Sharif University of Technology in 1996, and his MSc and PhD in Analytical Chemistry from Sharif University of Technology in 1998 and 2002, respectively. His research interests include analysis of real samples, separation by chromatographic techniques, analysis of surfactants, species preconcentration, and colorimetric sensors.

Mohammad Mahdi Bordbar received the BSC degree in applied chemistry from Kashan University in 2010, M. Sc. and pH.D. degrees in analytical chemistry from Yasouj University (2012) and Shiraz University (2018), respectively. His research is focused on fabrication of optical sensor array for food, environmental and biological applications.